HHS Public Access

Author manuscript

Nature. Author manuscript; available in PMC 2011 September 15.

Published in final edited form as:

Nature. 2011 March 3; 471(7336): 119–123. doi:10.1038/nature09755.

The RAG2 C-terminus suppresses genomic instability and lymphomagenesis

Ludovic Deriano[1], **Julie Chaumeil**[1], **Marc Coussens**[1], **Asha Multani**[2], **YiFan Chou**[1], **Alexander V. Alekseyenko**[3], **Sandy Chang**[4], **Jane A. Skok**[1,5], and **David B. Roth**[1]

[1]Department of Pathology, New York University School of Medicine, New York, NY 10016, USA.

[2]Department of Genetics, Department of Hematopathology, The M.D. Anderson Cancer Center, Houston, TX 77030, USA.

[3]Department of Medicine, Division of Clinical Pharmacology, Center for Health Informatics and Bioinformatics, New York University School of Medicine, USA.

[4]Department of Laboratory Medicine, Yale University School of Medicine, New Haven, CT 06520, USA.

[5]Department of Immunology and Molecular Pathology, Division of Infection and Immunity, University College London, London W1T 4JF, United Kingdom.

Abstract

Misrepair of DNA double-strand breaks (DSBs) produced by the V(D)J recombinase (the RAG1/RAG2 proteins) at *immunoglobulin* (*Ig*) and *T cell receptor* (*Tcr*) loci has been implicated in pathogenesis of lymphoid malignancies in humans[1] and in mice[2–7]. Defects in DNA damage response factors such as ATM and combined deficiencies in classical nonhomologous end joining (NHEJ) and p53 predispose to RAG-initiated genomic rearrangements and lymphomagenesis[2–11]. Although we showed previously that RAG1/RAG2 shepherd the broken DNA ends to classical NHEJ for proper repair[12,13], roles for the RAG proteins in preserving genomic stability remain poorly defined. Here we show that the RAG2 C-terminus, although dispensable for recombination[14,15], is critical for maintaining genomic stability. Thymocytes from *"core" Rag2* homozygotes (*Rag2*$^{c/c}$ mice) show dramatic disruption of *Tcrα/δ* locus integrity. Furthermore, all *Rag2*$^{c/c}$ *p53*$^{-/-}$ mice, unlike *Rag1*$^{c/c}$ *p53*$^{-/-}$ and *p53*$^{-/-}$ animals, rapidly develop thymic lymphomas bearing complex chromosomal translocations, amplifications, and deletions involving the *Tcrα/δ* and *Igh* loci. We also find these features in lymphomas from *Atm*$^{-/-}$ mice. We show that, like ATM-deficiency[3], core RAG2 severely destabilizes the RAG post-cleavage complex.

Correspondence to: david.roth@nyumc.org.

Contributions

L.D. and D.B.R. conceived the study and co-wrote the manuscript. L.D. designed the experiments. L.D., J.C. M.C. and A.M. performed the experiments. Y.C. provided assistance with the mouse colonies. A.V.A. performed the aCGH data analysis. J.A.S. and S.C. provided technical and conceptual support. J.C. and J.A.S revised the manuscript. All the authors read and approved the manuscript.

Competing financial interests

The authors declare no competing financial interests.

These results reveal a novel genome guardian role for RAG2 and suggest that similar “end release/end persistence” mechanisms underlie genomic instability and lymphomagenesis in *Rag2*$^{c/c}$ *p53*$^{-/-}$ and *Atm*$^{-/-}$ mice.

RAG mutations can cause specific defects in the joining stage of V(D)J recombination[12,13,16]. The “dispensable” RAG2 C-terminus (murine amino acids 1–383) is of particular interest: Loss of the RAG2 C-terminus impairs joining of substrates[17], increases levels of DSBs[17] that persist through the cell cycle[18], and increases accessibility of the broken DNA ends to alternative NHEJ[12,19]. Despite these defects, *Rag2*$^{c/c}$ mice are not lymphoma-prone.

We reasoned that *Rag2*$^{c/c}$ *p53*$^{-/-}$ double mutant mice might display genomic instability and lymphomagenesis, even in the context of intact classical NHEJ. Consistent with previous reports[15], our *Rag2*$^{c/c}$ mice displayed partial developmental blocks in B and T lymphopoiesis because of a selective V-to-DJ rearrangement defect (Supplementary Fig. 1). *Rag2*$^{c/c}$ animals, observed for up to one year, showed no obvious signs of tumorigenesis (Fig. 1a and data not shown). As expected[20], approximately two-thirds of *p53*$^{-/-}$ mice developed thymic lymphoma at an average age of ≈ 23 weeks (mean survival = 22.8 weeks) (Fig. 1a, b). Similar findings in RAG/p53 deficient mice[21] demonstrate that RAG-initiated DSBs are not critical initiators of lymphomagenesis in p53-deficient mice. In sharp contrast, 100% (n = 25) of our *Rag2*$^{c/c}$ *p53*$^{-/-}$ mice died within 16 weeks (mean survival = 12.1 weeks) with aggressive thymic lymphomas (Fig. 1a, b, c). Tumor cells were highly proliferative and expressed cell surface CD4 and CD8 (Supplementary Fig. 2), with little or no surface TCR (CD3ε or TCRβ) (data not shown), indicating that these tumors originate from immature thymocytes. Tumors with highly proliferating lymphoblasts were detected in 4- to 6-week-old *Rag2*$^{c/c}$ *p53*$^{-/-}$ thymi, but not in other organs (data not shown), confirming their thymic origin. *Rag2*$^{c/c}$ *p53*$^{-/-}$ tumors generally displayed one or a few predominant Dβ1-Jβ1 or Dβ2-Jβ2 rearrangements, indicating a clonal or oligoclonal origin (Supplementary Fig. 3).

We next examined genomic stability in lymphomas from *Rag2*$^{c/c}$ *p53*$^{-/-}$ mice, first by analysis of Giemsa stained metaphase spreads prepared from 12 *Rag2*$^{c/c}$ *p53*$^{-/-}$ and two *p53*$^{-/-}$ thymic lymphomas (Supplementary Table 1). Wild-type thymocytes showed almost no abnormal metaphases (0% to 3%) (Supplementary Table 1). In contrast, *p53*$^{-/-}$ and *Rag2*$^{c/c}$ *p53*$^{-/-}$ tumors harbored a variety of cytogenetic aberrations (aberrant metaphases: 8% to 94%), including aneuploidy, chromosome breaks, and chromosome fusions (Supplementary Table 1). We analyzed three *Rag2*$^{c/c}$ *p53*$^{-/-}$ thymic lymphomas using spectral (1790T and 1745T) and G-band (1779T) karyotyping (Fig. 2). We observed recurrent translocations involving chromosomes that harbor *Tcr* (Chr. 14 and 6) and *Ig* (Chr. 12, 6 and 16) loci, suggesting that these might have been initiated by RAG-generated breaks. Moreover, all three lymphomas harbored translocations of the *Igh* locus-containing chromosome 12 and/or the *Tcrα/δ* locus-containing chromosome 14, loci which rearrange in thymocytes[22]. Analysis of lymphoma 1779T revealed a C12;14 translocation (Fig. 2). These results suggest that *Rag2*$^{c/c}$ *p53*$^{-/-}$ T cell tumors harbor clonal translocations involving the

Tcrα/δ and *Igh* loci, as seen in T cell lymphomas from ataxia-telangiectasia patients and *Atm*$^{-/-}$ mice[7,8,10,11], rearrangements not observed in *p53*$^{-/-}$ lymphomas[21,23].

To confirm the involvement of the *Tcrα/δ* locus in chromosome translocations, we performed DNA-fluorescent in situ hybridization (DNA-FISH) analyses on metaphases from *Rag2*$^{c/c}$ *p53*$^{-/-}$ thymic lymphomas (2489T and 2805T) using probes centromeric (*Tcrα/δ V*) and telomeric (*Tcrα/δ C*) to the *Tcrα/δ* locus plus a paint for chromosome 14 (Fig. 3a). In both tumors, breakpoints within the *Tcrα/δ* locus of one of the two chromosomes 14 resulted in amplification of the *Tcrα/δ V* region (Fig. 3a). The telomeric fragment (including *Tcrα/δ C*) was either translocated (2489T), or lost (2805T) (Fig. 3a). DNA-FISH analysis of tumors 1790T and 1779T (from Fig. 2) using *Tcrα/δ C* and *V* probes also confirmed translocation of chromosome 14 with breakpoints within the *Tcrα/δ* locus, although without obvious amplification (Supplementary Fig. 4).

We next performed DNA-FISH on *Rag2*$^{c/c}$ *p53*$^{-/-}$ thymic lymphomas 2489T and 2805T using probes centromeric (*Igh C*) and telomeric (*Igh V*) to the *Igh* locus along with a chromosome 12 paint (Fig. 3b). In both lymphomas, one chromosome 12 showed translocation with another chromosome, with accompanying loss of both *Igh C* and *V* signals (Fig. 3b). This could result from RAG-induced breaks with loss of the telomeric end of the chromosome (including *Igh V*) and loss of the *Igh C* region by end degradation before fusion to the partner chromosome, as previously reported in *Atm*$^{-/-}$ mouse T cells[8]. Moreover, dual chromosome 12 and 14 paint analysis showed a C12;14 translocation in lymphoma 2489T (Fig 3b). In contrast to *Rag2*$^{c/c}$ *p53*$^{-/-}$ lymphomas, DNA-FISH on metaphases from one *p53*$^{-/-}$ thymic lymphoma (6960T) indicated that both *Tcrα/δ* and *Igh* loci were intact (Supplementary Fig. 5), consistent with previous work[21].

We next performed array-based comparative genomic hybridization (a-CGH) analysis on genomic DNA from five *Rag2*$^{c/c}$ *p53*$^{-/-}$ thymic lymphomas (2489T, 2805T, 1348T, 1779T, 1780T). We observed loss or gain of a region within the *Tcrα/δ* and *Igh* loci, reflecting V(D)J recombination (Supplementary Fig. 6). All five *Rag2*$^{c/c}$ *p53*$^{-/-}$ lymphomas examined showed substantial amplification of a common region on chromosome 14, centromeric of the *Tcrα/δ* locus (Supplementary Fig. 6a), in agreement with our FISH analyses (Fig. 3a). We also observed loss of a common region on chromosome 12, telomeric of the *Igh* locus in all five *Rag2*$^{c/c}$ *p53*$^{-/-}$ thymic lymphomas analyzed (Supplementary Fig. 6b). Tumors 1779T, 2489T and 2805 also showed loss of a large region centromeric of the *Igh* locus, likely reflecting DNA-end degradation before fusion to the partner chromosome (Fig. 2; Fig. 3a, b; Supplementary Fig. 6b). In contrast, aCGH analysis of *p53*$^{-/-}$ thymic lymphoma 6960T failed to reveal amplification centromeric to the *Tcrα/δ* locus or deletion telomeric to the *Igh* locus (Supplementary Fig. 7a, b), in agreement with our FISH analysis (Supplementary Fig. 5) and previous data[23].

Blocking lymphocyte development in early stages can lead to persistent RAG activity, which, in the absence of p53, can provoke lymphomagenesis[23]. To investigate whether the partial developmental block in *Rag2*$^{c/c}$ thymocytes[15] is sufficient to produce genomic instability and lymphomagenesis, we crossed *core Rag1* knock-in animals, which display diminished recombination and a strong block in B and T cell development[14,24]

(Supplementary Fig. 1), into a p53 deficient background. *Rag1*$^{c/c}$ *p53*$^{-/-}$ mice survived at an average age of 18.7 weeks (Supplementary Fig. 8a), barely distinguishable from *p53*$^{-/-}$ mice. Also like *p53*$^{-/-}$ mice, only two-thirds of *Rag1*$^{c/c}$ *p53*$^{-/-}$ mice developed thymic lymphomas (Supplementary Fig. 8b). Futhermore, metaphase DNA-FISH analyses on two *Rag1*$^{c/c}$ *p53*$^{-/-}$ thymic lymphomas (8383T and 8411T) (Supplementary Fig. 9) and aCGH analysis on genomic DNA from four *Rag1*$^{c/c}$ *p53*$^{-/-}$ thymic lymphomas (8315T, 8333T, 8383T, 8411T) (Supplementary Fig. 10) showed no evidence of recurrent translocations, genomic amplification or genomic deletion at chromosome 14 and chromosome 12. The genomic instability observed in *Rag2*$^{c/c}$ *p53*$^{-/-}$ thymic lymphomas is therefore associated specifically with loss of the RAG2 C-terminus, and does not result from the developmental block in *core RAG2* homozygotes.

We next asked whether core RAG2 promotes genomic instability in the presence of p53 by using three-dimensional interphase DNA-FISH to examine the integrity of *Tcrα/δ* locus (Fig. 3c) in *Rag2*$^{c/c}$ double positive (DP) thymocytes. The two alleles appeared as two pairs of signals (*Tcrα/δ V* and *Tcrα/δ C*, mapping the two ends of the locus) in most (>98%) *wild-type* and *p53*$^{-/-}$ DP thymocytes (Fig. 3d and Supplementary Fig. 11), indicating that p53 deficiency alone does not disrupt the integrity of the *Tcrα/δ* locus, as expected[25]. In contrast, *Rag2*$^{c/c}$ DP thymocytes displayed a three- to five-fold increase in the number of cells showing loss of at least one signal (Fig. 3c, d and Supplementary Fig. 11). These results suggest that core RAG2 promotes genomic instability at the *Tcrα/δ* locus, a phenotype similar to that previously reported in *Atm*$^{-/-}$ and *53bp1*$^{-/-}$ animals[9,25].

We noted that both *Rag2*$^{c/c}$ *p53*$^{-/-}$ and *Atm* $^{-/-}$ mice feature RAG-dependent genomic instability at the *Tcrα/δ* and *Igh* loci, with development of pro-T cell lymphomas bearing clonal translocations, including 12/14 translocations[2,3,7–11]. To determine whether *Atm*$^{-/-}$ thymic lymphomas also harbor amplification close to the *Tcrα/δ* locus, we performed DNA-FISH analysis for *Tcrα/δ* and chromosome 14 on metaphases from one *Atm*$^{-/-}$ thymic lymphoma (10375T) (Supplementary Fig. 12a). Both chromosomes 14 showed translocations with breakpoints within the *Tcrα/δ* locus, and amplification of the *Tcrα/δ V* region on one allele (Supplementary Fig. 12a), results that were confirmed by array-CGH analysis (Supplementary Fig. 12b). We also observed loss of DNA at a distal region of chromosome 12, near the *Igh* locus (Supplementary Fig. 12b), as in *Rag2*$^{c/c}$ *p53*$^{-/-}$ lymphomas (Fig. 3 a,b; Supplementary Fig. 6). These data agree with recent analysis of thymic lymphomas from ATM-deficient mice[7]. Thymic lymphomas that arise in other mutant backgrounds such as p53, core RAG1/p53 (Supplementary Fig 8, 9, 10), Eβ/p53 or H2AX/p53 lack recurrent amplifications of chromosome 14 regions and/or recurrent chromosome 12/14 translocations, and thus appear to arise from distinct mechanisms.

Our data reveal a novel *in vivo* function for the RAG2 C-terminus in promoting genomic stability. How does core RAG2 allow genomic instability? We hypothesized that core RAG2, like the absence of ATM[3], destabilizes the post-cleavage complex. To investigate this, we generated RAG-signal end complexes by *in vitro* cleavage and challenged them at increasing temperatures, followed by gel electrophoresis (Fig. 4). Complexes containing full length RAG2 did not release 50% of signal ends until 55°C (Fig. 4b, c), as expected[13,26]. In contrast, core RAG2-containing complexes displayed statistically significant instability at

lower temperatures, with 50% end release at 37°C (Fig. 4b, c). To examine the post-cleavage complex *in vivo*, we analyzed inversional recombination, which requires coordination of all four DNA ends. Decreased inversional recombination and increased formation of hybrid joints (generated by joining of a coding end to a signal end, in this case revealing defects in formation of four-ended inversion products) has been reported in ATM- and MRE11 complex-deficient cells[3,27,28]. As expected[3,28], we observed increased hybrid joint formation at the *Igκ* locus (*Vκ6-23* to *Jκ1*) in $Atm^{-/-}$ and $Nbs^{\Delta B/\Delta B}$ splenocytes (Supplementary Fig. 13). Importantly, we observed increased *Vκ6-23*-to-*Jκ1* hybrid joints in $Rag2^{c/c}$ splenocytes, compared to their wild-type and $Rag2^{c/+}$ counterparts (Supplementary Fig. 13). These results are supported by the observation that $Rag2^{c/c}$ lymphocytes exhibit defects in inversional recombination[15]. Together, these data support our hypothesis that core RAG2 impairs the stability of the RAG post-cleavage complex *in vitro* and *in vivo*.

Our data support a common model for genomic instability in $Rag2^{c/c}$ $p53^{-/-}$ and $Atm^{-/-}$ mice: premature release of RAG-generated DSBs from the RAG post-cleavage complex allows ends to escape the normal joining mechanisms, to persist, and to be potentially joined by alternative NHEJ, a pathway permissive for chromosome tranlocations and amplification[4,29]. Both end release and end persistence are promoted by ATM deficiency[2,3], likely because ATM both stabilizes the RAG post-cleavage complex[3] and activates p53-dependent checkpoints/apoptosis. In $Rag2^{c/c}$ $p53^{-/-}$ mice, end persistence might be augmented by ongoing RAG activity through the cell cycle resulting from impaired degradation of core RAG2, which lacks the cell-cycle regulated degradation motif[18,30].

The complete penetrance, rapid development of lymphoma, and extraordinary degree of RAG-mediated genomic instability make $Rag2^{c/c}$ $p53^{-/-}$ mice an attractive model for investigating the spectrum of somatic genome rearrangements underlying lymphomagenesis.

Methods Summary

Mice

Mice were bred in the NYU SPF facility; animal care was approved by the NYU SoM Animal Care and Use Committee (Protocol # 090308-2).

Analysis of tumor cells

Lymphoid tumors were analyzed by flow cytometry with antibodies against surface B- and T- cell markers. Metaphases were prepared and analyzed as described in Full Methods.

FISH and image analysis

DNA FISH was performed using BAC probes as described in Full Methods. Interphase FISH was performed on double positive thymocytes isolated by cell sorting according to protocols described in Full Methods. Images were obtained by confocal microscopy on a Leica SP5 AOBS system (Acousto-Optical Beam Splitter), with optical sections separated by 0.3 micrometers. Images were analyzed using Image J software. Metaphase spreads were imaged by fluorescent microscopy on a Zeiss Imager Z2 Metasystems METAFER 3.8

system and analyzed using ISIS software. Statistical analysis of image parameters was performed using the two-tailed Fisher's exact test.

Biochemical end release assay

The stability of RAG-signal end complexes was measured as described in Full Methods. Briefly, RAG cleavage reactions were aliquoted into microfuge tubes and incubated at the indicated temperatures for 30 minutes, followed by polyacrylamide gel electrophoresis. DNA was stained using SYBR Safe DNA Gel Stain (Invitrogen) and quantified with Quantity One software (Biorad). Student's T-test assuming equal variance was used to calculate statistical significance.

aCGH analysis

For CGH, genomic DNA from mouse thymic lymphomas was profiled against matched thymic DNA from wild type mice. aCGH experiments were performed on two color Agilent 244A Mouse Genome Microarrays. Data analysis was performed as described in Full Methods.

Full Methods

Mice

We obtained *wild type* (Taconic), *Rag2*$^{c/c15}$, *Rag1*$^{c/c}$ [24], *p53*$^{-/-}$ (The Jackson Laboratory[20]) and *Atm*$^{-/-}$ (The Jackson Laboratory[11]) mice for this study. *Rag2*$^{c/c}$ or *Rag1*$^{c/c}$ mice were bred with p53-deficient mice to generate doubly deficient mice. Genotyping of these mutants was performed by PCR of tail DNA as described in the relevant references[11,15,20,24].

Characterization of tumor cells and metaphase preparation

Lymphoid tumors were analyzed by flow cytometry with antibodies against surface B-cell (CD43, B220, IgM) and T-cell (CD4, CD8, CD3, TCRβ) markers. FACS analysis employed a BD LSRII flow cytometer (BD Biosciences) equipped with FacsDiVa and FlowJo. For metaphase preparation, tumor cells were prepared as previously described[31,32]. Briefly, primary tumor cells were grown in complete RPMI media for 4 hours and exposed to Colcemid (0.04 μg/ml, GIBCO, Karyo max Colcemid solution) for two hours at 37°C. Then, cells were incubated in KCl 75mM for 15 minutes at 37°C, fixed in fixative solution (75% methanol/25% acetic acid) and washed three times in the fixative. Cell suspension was dropped onto pre-chilled glass slides and air-dried for further analysis.

G-banding and Spectral Karyotyping

Optimally aged slides were treated for the induction of G-banding following the routine procedure[33]. Spectral karyotyping was performed using the mouse chromosome SKY probe Applied Spectral Imaging (ASI, Vista, CA, USA) according to the manufacturer's instructions to determine chromosomal rearrangements in the tumor samples. The slides were analyzed using Nikon Eclipse 80i microscope. G-banding as well as SKY images were captured and karyotyped using ASI system.

DNA FISH probes—BAC probes for the *Igh* and *Tcrα/δ* loci were labeled by nick-translation and prepared as previously described[34,35]. For the *Igh* locus, BAC 199 (*Igh C*) and BAC RP24-386J17 (*Igh V*) were labeled in Alexa Fluor 594 and 488 respectively (Molecular probes). For the *Tcrα/δ* locus, BAC RP23-304L21 (*Tcrα/δ V*) and RP-23 255N13 (*Tcrα/δ C*) were labeled in Alexa Fluor 488 or 594. StarFISH-concentrated mouse FITC or Cy3 chromosome 12 or 14 paints were prepared following supplier's instructions (Cambio). BAC probes were resuspended in hybridization buffer (10% dextran sulfate, 5X Denharts solution, 50% formamide) or in paint hyb buffer, denatured for 5 min at 95°C and pre-annealed for 45 min at 37°C before hybridization on cells.

DNA FISH on metaphase spreads—Slides were dehydrated in ethanol series, denatured in 70% formamide/2x SSC (pH 7–7.4) for 1 min 30s at 75°C, dehydrated again in cold ethanol series, and hybridized with probes o/n at 37°C in a humid chamber. Slides were then washed twice in 50% formamide/2x SSC and twice in 2x SSC for 5 min at 37°C each. Finally, cells were mounted in ProLong Gold (Invitrogen) containing DAPI to counterstain total DNA.

DNA FISH on interphase nuclei—Double-positive thymocytes were isolated from total thymi on a Beckman-Coulter MoFlo cell sorter as $Thy1.2^{+}CD4^{+}CD8^{+}$ cells using the following antibodies: PE-Cy7-coupled anti-CD90.2 (Thy1.2; 53-2.1), APC-coupled anti-CD4 (L3T4) and FITC-coupled anti-CD8 (53-6.7). Cells were washed two times in 1X PBS and dropped onto poly-L-lysine-coated coverslips. For 3-dimensional DNA-FISH analyses we used a protocol for immunofluorescence / DNA-FISH previously described[34,35], with protein detection step omitted. Briefly, cells were fixed in 2% paraformaldehyde / 1X PBS for 10 min at RT, permeabilized in 0.4% Triton / 1X PBS for 5 min on ice, incubated with 0.01 mg/ml Rnase A for one hour at 37°C and permeabilized again in 0.7% Triton / 0.1M HCl for 10 min on ice. Cells were then denatured in 1.9M HCl for 30 minutes at RT, rinsed in cold 1X PBS and hybridized overnight with probes at 37°C in a humid chamber. Cells were then rinsed in 2X SSC at 37°C, 2X SCC at RT and 1X SSC at RT, 30 min each. Finally, cells were mounted in ProLong Gold (Invitrogen) containing DAPI to counterstain total DNA.

Biochemical end release assay—End release assay to measure the stability of the signal-end complexes was performed as previously described[26]. For RAG-mediated cleavage, 100ng of recombination substrate (PCR product from pJH289) was incubated for 3 hours at 37°C with 200ng purified RAG protein and 200ng of purified recombinant HMGB1 in a buffer containing 50mM Hepes (pH 8.0), 25mM KCl, 4mM NaCl, 1mM DTT, 0.1mg BSA, 5mM $CaCl_2$ and 5mM $MgCl_2$. Reactions were then aliquoted into microfuge tubes and incubated at different temperatures, or treated with stop buffer [10mM Tris (pH 8.0), 10mM EDTA, 0.2% SDS, 0.35mg/ml proteinase K (Sigma Aldrich)] for 30 minutes and then ran out on 4–20% acrylamide TBE gels (Invitrogen).

aCGH analysis—aCGH experiments were performed on two color Agilent 244A Mouse Genome Microarray. After internal Agilent quality control, the collected data was background substracted and normalized using Loess Method[36]. We used circular binary

segmentation method to define regions of copy number alteration versus the control[37] and applied cghMCR method for extraction of altered minimum common regions between the samples[38]. The analyses and visualizations were performed using R statistical program [R development Core Team, 2009].

Supplementary Material

Refer to Web version on PubMed Central for supplementary material.

Acknowlegments

We thank Mark Schlissel for the generous gift of *core Rag2* mice, Fred Alt for the generous gift of *core Rag1* mice and Susannah Hewitt for the *Igh* BAC probes. D.B.R. was supported by NIH Roadmap Initiative in Nanomedicine through a Nanomedicine Development Center award (1PN2EY018244), NIH grant CA104588, and the Irene Diamond Fund. L.D. is a Fellow of The Leukemia and Lymphoma Society. A.V.A. was supported in part by grant 1UL1RR029893 from the National Center for Research Resources, National Institutes of Health. J.A.S. was supported by an R01GM086852, a NIH Challenge grant NCI R01CA145746-01 and the Leukemia and Lymphoma Scholar Award.

References

1. Kuppers R, Dalla-Favera R. Mechanisms of chromosomal translocations in B cell lymphomas. Oncogene. 2001; 20:5580–5594. [PubMed: 11607811]
2. Callen E, et al. ATM prevents the persistence and propagation of chromosome breaks in lymphocytes. Cell. 2007; 130:63–75. [PubMed: 17599403]
3. Bredemeyer AL, et al. ATM stabilizes DNA double-strand-break complexes during V(D)J recombination. Nature. 2006; 442:466–470. [PubMed: 16799570]
4. Zhu C, et al. Unrepaired DNA breaks in p53-deficient cells lead to oncogenic gene amplification subsequent to translocations. Cell. 2002; 109:811–821. [PubMed: 12110179]
5. Gao Y, et al. Interplay of p53 and DNA-repair protein XRCC4 in tumorigenesis, genomic stability and development. Nature. 2000; 404:897–900. [PubMed: 10786799]
6. Difilippantonio MJ, et al. DNA repair protein Ku80 suppresses chromosomal aberrations and malignant transformation. Nature. 2000; 404:510–514. [PubMed: 10761921]
7. Zha S, et al. ATM-deficient thymic lymphoma is associated with aberrant tcrd rearrangement and gene amplification. J Exp Med. 2010; 207:1369–1380. [PubMed: 20566716]
8. Callen E, et al. Chimeric IgH-TCRalpha/delta translocations in T lymphocytes mediated by RAG. Cell Cycle. 2009; 8:2408–2412. [PubMed: 19556863]
9. Matei IR, et al. ATM deficiency disrupts Tcra locus integrity and the maturation of CD4+CD8+ thymocytes. Blood. 2007; 109:1887–1896. [PubMed: 17077325]
10. Liyanage M, et al. Abnormal rearrangement within the alpha/delta T-cell receptor locus in lymphomas from Atm-deficient mice. Blood. 2000; 96:1940–1946. [PubMed: 10961898]
11. Barlow C, et al. Atm-deficient mice: A paradigm of ataxia telangiectasia. Cell. 1996; 86:159–171. [PubMed: 8689683]
12. Corneo B, et al. Rag mutations reveal robust alternative end joining. Nature. 2007; 449:483–486. [PubMed: 17898768]
13. Lee GS, Neiditch MB, Salus SS, Roth DB. RAG proteins shepherd double-strand breaks to a specific pathway, suppressing error-prone repair, but RAG nicking initiates homologous recombination. Cell. 2004; 117:171–184. [PubMed: 15084256]
14. Jones JM, Simkus C. The roles of the RAG1 and RAG2 "non-core" regions in V(D)J recombination and lymphocyte development. Arch Immunol Ther Exp (Warsz). 2009; 57:105–116. [PubMed: 19333736]

15. Liang HE, et al. The "dispensable" portion of RAG2 is necessary for efficient V-to-DJ rearrangement during B and T cell development. Immunity. 2002; 17:639–651. [PubMed: 12433370]
16. Qiu JX, Kale SB, Yarnell Schultz H, Roth DB. Separation-of-function mutants reveal critical roles for RAG2 in both the cleavage and joining steps of V(D)J recombination. Mol Cell. 2001; 7:77–87. [PubMed: 11172713]
17. Steen SB, Han J-O, Mundy C, Oettinger MA, Roth DB. Roles of the "dispensable" portions of RAG-1 and RAG-2 in V(D)J recombination. Molecular and Cellular Biology. 1999; 19:3010–3017. [PubMed: 10082568]
18. Curry JD, Schlissel MS. RAG2's non-core domain contributes to the ordered regulation of V(D)J recombination. Nucleic Acids Res. 2008; 36:5750–5762. [PubMed: 18776220]
19. Talukder SR, Dudley DD, Alt FW, Takahama Y, Akamatsu Y. Increased frequency of aberrant V(D)J recombination products in core RAG-expressing mice. Nucl. Acids Res. 2004; 32:4539–4549. [PubMed: 15328366]
20. Jacks T, et al. Tumor spectrum analysis in p53-mutant mice. Curr Biol. 1994; 4:1–7. [PubMed: 7922305]
21. Liao MJ, et al. No requirement for V(D)J recombination in p53-deficient thymic lymphoma. Mol Cell Biol. 1998; 18:3495–3501. [PubMed: 9584189]
22. Forster A, Hobart M, Hengartner H, Rabbitts TH. An immunoglobulin heavy-chain gene is altered in two T-cell clones. Nature. 1980; 286:897–899. [PubMed: 6774263]
23. Haines BB, et al. Block of T cell development in P53-deficient mice accelerates development of lymphomas with characteristic RAG-dependent cytogenetic alterations. Cancer Cell. 2006; 9:109–120. [PubMed: 16473278]
24. Dudley DD, et al. Impaired V(D)J recombination and lymphocyte development in core RAG1-expressing mice. J Exp Med. 2003; 198:1439–1450. [PubMed: 14581608]
25. Difilippantonio S, et al. 53BP1 facilitates long-range DNA end-joining during V(D)J recombination. Nature. 2008; 456:529–533. [PubMed: 18931658]
26. Arnal SM, Holub AJ, Salus SS, Roth DB. Non-consensus heptamer sequences destabilize the RAG post-cleavage complex, making ends available to alternative DNA repair pathways. Nucleic Acids Res. 2010; 38:2944–2954. [PubMed: 20139091]
27. Helmink BA, et al. MRN complex function in the repair of chromosomal Rag-mediated DNA double-strand breaks. J Exp Med. 2009
28. Deriano L, Stracker TH, Baker A, Petrini JH, Roth DB. Roles for NBS1 in alternative nonhomologous end-joining of V(D)J recombination intermediates. Mol Cell. 2009; 34:13–25. [PubMed: 19362533]
29. Simsek D, Jasin M. Alternative end-joining is suppressed by the canonical NHEJ component Xrcc4-ligase IV during chromosomal translocation formation. Nat Struct Mol Biol. 2010
30. Li Z, Dordai DI, Lee J, Desiderio S. A conserved degradation signal regulates RAG-2 accumulation during cell division and links V(D)J recombination to the cell cycle. Immunity. 1996; 5:575–589. [PubMed: 8986717]
31. Theunissen JW, Petrini JH. Methods for studying the cellular response to DNA damage: influence of the Mre11 complex on chromosome metabolism. Methods Enzymol. 2006; 409:251–284. [PubMed: 16793406]
32. Multani AS, et al. Caspase-dependent apoptosis induced by telomere cleavage and TRF2 loss. Neoplasia. 2000; 2:339–345. [PubMed: 11005568]
33. Pathak S. Chromosome banding techniques. J Reprod Med. 1976; 17:25–28. [PubMed: 59808]
34. Hewitt SL, et al. RAG-1 and ATM coordinate monoallelic recombination and nuclear positioning of immunoglobulin loci. Nat Immunol. 2009; 10:655–664. [PubMed: 19448632]
35. Skok JA, et al. Reversible contraction by looping of the Tcra and Tcrb loci in rearranging thymocytes. Nat Immunol. 2007; 8:378–387. [PubMed: 17334367]
36. Yang YH, et al. Normalization for cDNA microarray data: a robust composite method addressing single and multiple slide systematic variation. Nucleic Acids Res. 2002; 30:e15. [PubMed: 11842121]

37. Olshen AB, Venkatraman ES, Lucito R, Wigler M. Circular binary segmentation for the analysis of array-based DNA copy number data. Biostatistics. 2004; 5:557–572. [PubMed: 15475419]

38. Aguirre AJ, et al. High-resolution characterization of the pancreatic adenocarcinoma genome. Proc Natl Acad Sci U S A. 2004; 101:9067–9072. [PubMed: 15199222]

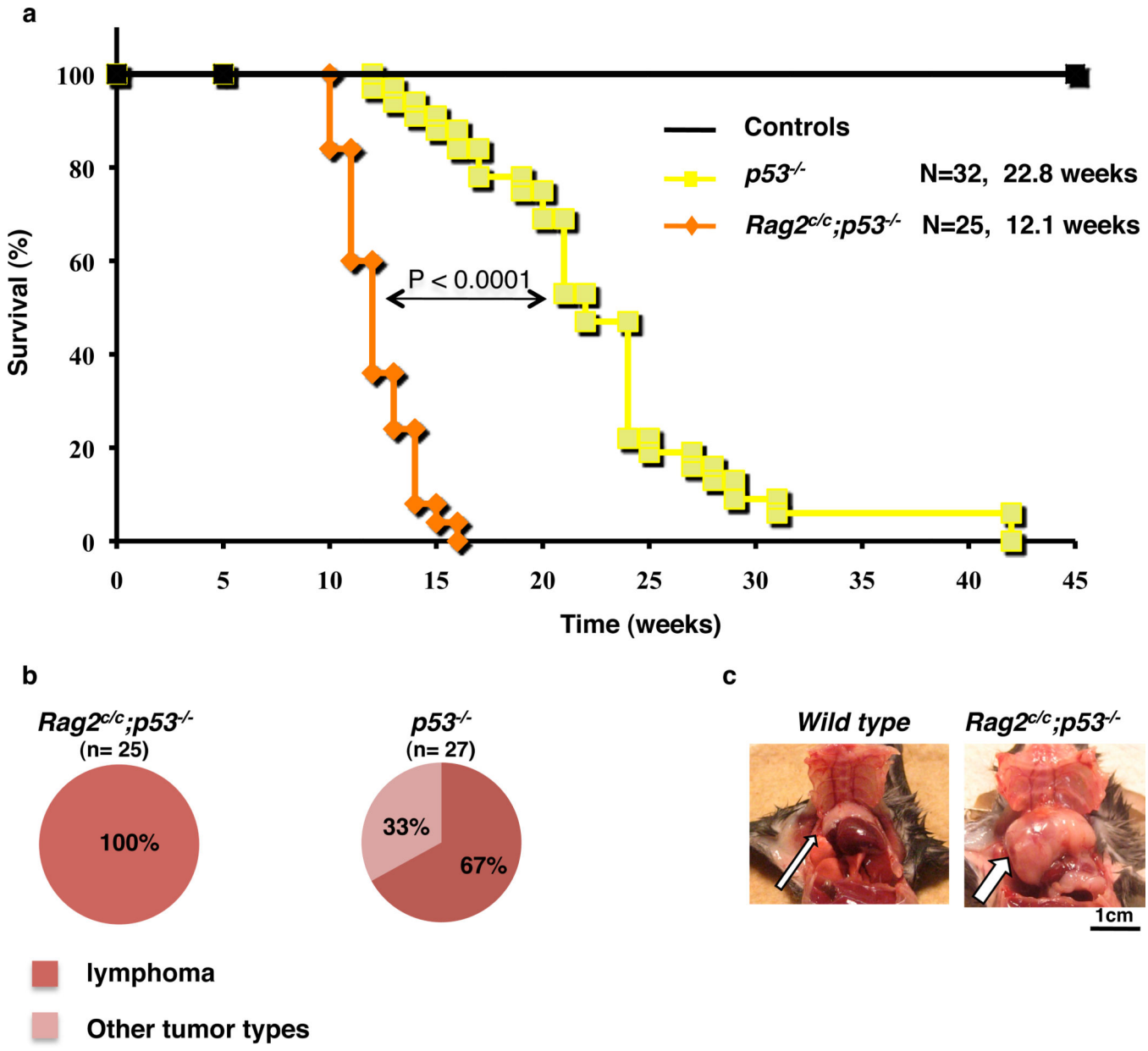

Figure 1. The C-terminus of RAG2 is a tumor suppressor in developing thymocytes

a. Kaplan-Meier tumor-free survival analysis for cohorts of control (*WT*, n=12 and *Rag2*$^{c/c}$, n=19), *p53*$^{-/-}$ (n=32) and *Rag2*$^{c/c}$ *p53*$^{-/-}$ (n=25) mice. Animals were monitored for 50 weeks. The average age of death in weeks is shown for *p53*$^{-/-}$ (22.8 weeks) and *Rag2*$^{c/c}$ *p53*$^{-/-}$ (12.1 weeks) genotypes with the *P*-value determined by the Wilcoxon rank sum test. **b.** Pie chart showing the tumor spectrum observed for *Rag2*$^{c/c}$ *p53*$^{-/-}$ (n=25) and *p53*$^{-/-}$ mice (n=27). All *Rag2*$^{c/c}$ *p53*$^{-/-}$ animals (n=25) showed enlarged thymus. *p53*$^{-/-}$ animals showed either enlarged thymus and/or spleen (n=18) or other non lymphoid tumor mass (n=9). **c.** Physical appearance of normal thymus (*wild type*) and thymic lymphoma (*Rag2*$^{c/c}$ *p53*$^{-/-}$, arrow) of 3-month-old animals.

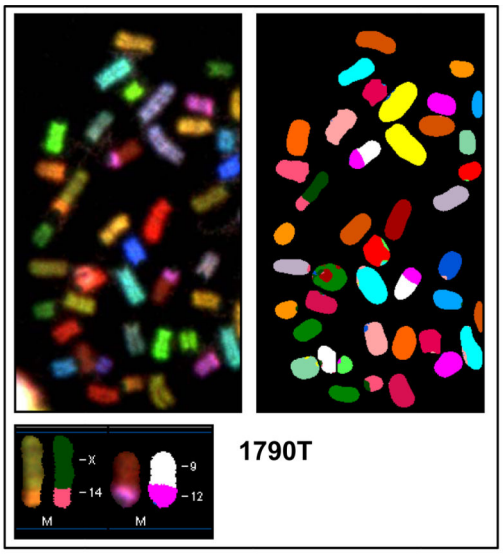

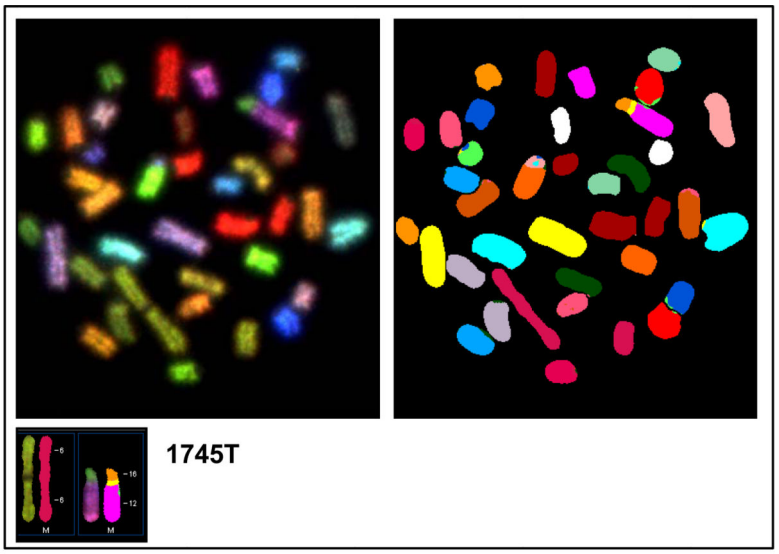

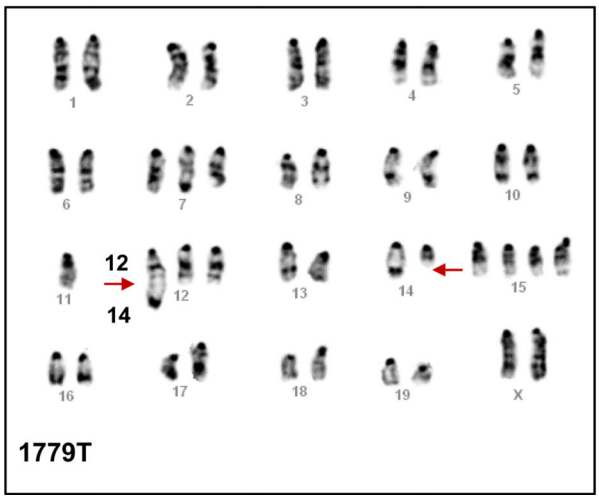

Tumor #	Genotype	Translocations*	Frequency
1790	*Rag2*$^{c/c}$;*p53*$^{-/-}$	t(9;12)	7/8
		t(X;14)	4/8
1745	*Rag2*$^{c/c}$;*p53*$^{-/-}$	t(16;12)	3/9
		t(6;6)	3/9
1779	*Rag2*$^{c/c}$;*p53*$^{-/-}$	t(12;14)	14/17

Figure 2. *Rag2*$^{c/c}$ *p53*$^{-/-}$ thymic lymphomas display recurrent translocations involving chromosomes that harbor antigen-receptor loci

Representative images of spectral karyotyping (1790T and 1745T) and G-band karyotyping (1779T) analysis of three *Rag2*$^{c/c}$ *p53*$^{-/-}$ T cell lymphomas. Metaphase number analyzed and translocations for each tumor sample are listed in the table.*All three tumors harbor clonal translocations involving chromosomes that carry *Tcr* (Chr.14: *Tcrα/δ*; Chr.6:*Tcrβ*) and/or *Ig* (Chr.12:*Igh*; Chr.6:*Igκ*; Chr.16:*Igλ*) loci.

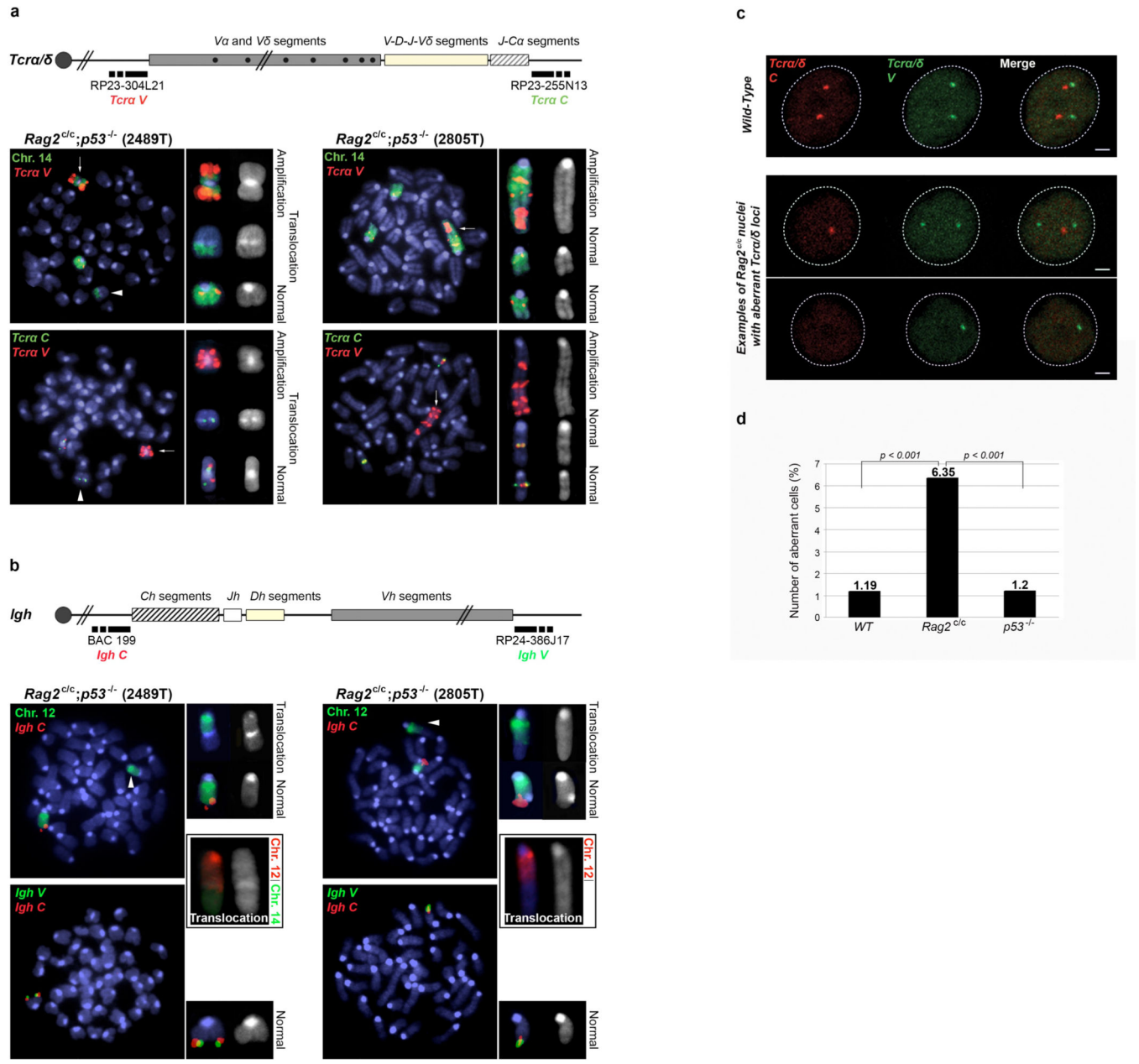

Figure 3. *Rag2*$^{c/c}$ *p53*$^{-/-}$ thymocytes display *Tcrα/δ* and *Igh*-associated genomic instability

a. Top panel: schematic of the *Tcrα/δ* locus, with positions of the BACs used for generation of DNA FISH probes indicated. Bottom panels: representative metaphases from two *Rag2*$^{c/c}$ *p53*$^{-/-}$ thymic lymphomas using the *Tcrα/δ V* BAC probe (red signal) combined with chromosome 14 paint (green signal, top row) or with the *Tcrα/δ C* BAC probe (green signal, bottom row). Arrows point the amplification of the *Tcrα/δ V* region, arrow heads point the translocated chromosome 14. **b.** Top panel: schematic of the *Igh* locus, with positions of the BACs used for generation of DNA FISH probes indicated. Bottom panels: representative metaphases from the same two *Rag2*$^{c/c}$ *p53*$^{-/-}$ thymic lymphomas using the *Igh C* BAC probe (red signal) combined with chromosome 12 paint (green signal, top row), or with the *Igh V* BAC probe (green signal, bottom row). Combination of chromosome 12 (red) and

chromosome 14 (green) paints is shown for both tumors in black boxes. Arrow heads point the translocated chromosome 12. **c.** Examples of confocal sections of three-dimensional *Tcrα/δ* DNA FISH on freshly isolated *wild-type* (top row) or *Rag2*$^{c/c}$ (bottom rows) double positive thymocytes. *Tcrα/δ V* (Green) and *C* (Red) BAC probes were used. Scale bar = 1μm. **d.** Representative experiment showing the frequency at which *Tcrα/δ V* and/or *Tcrα/δ C* signals are lost in *wild-type*, *p53*$^{-/-}$ and *Rag2*$^{c/c}$ thymocytes (n>200, see Supplementary Fig. 11 for additional experiments and statistical analysis).

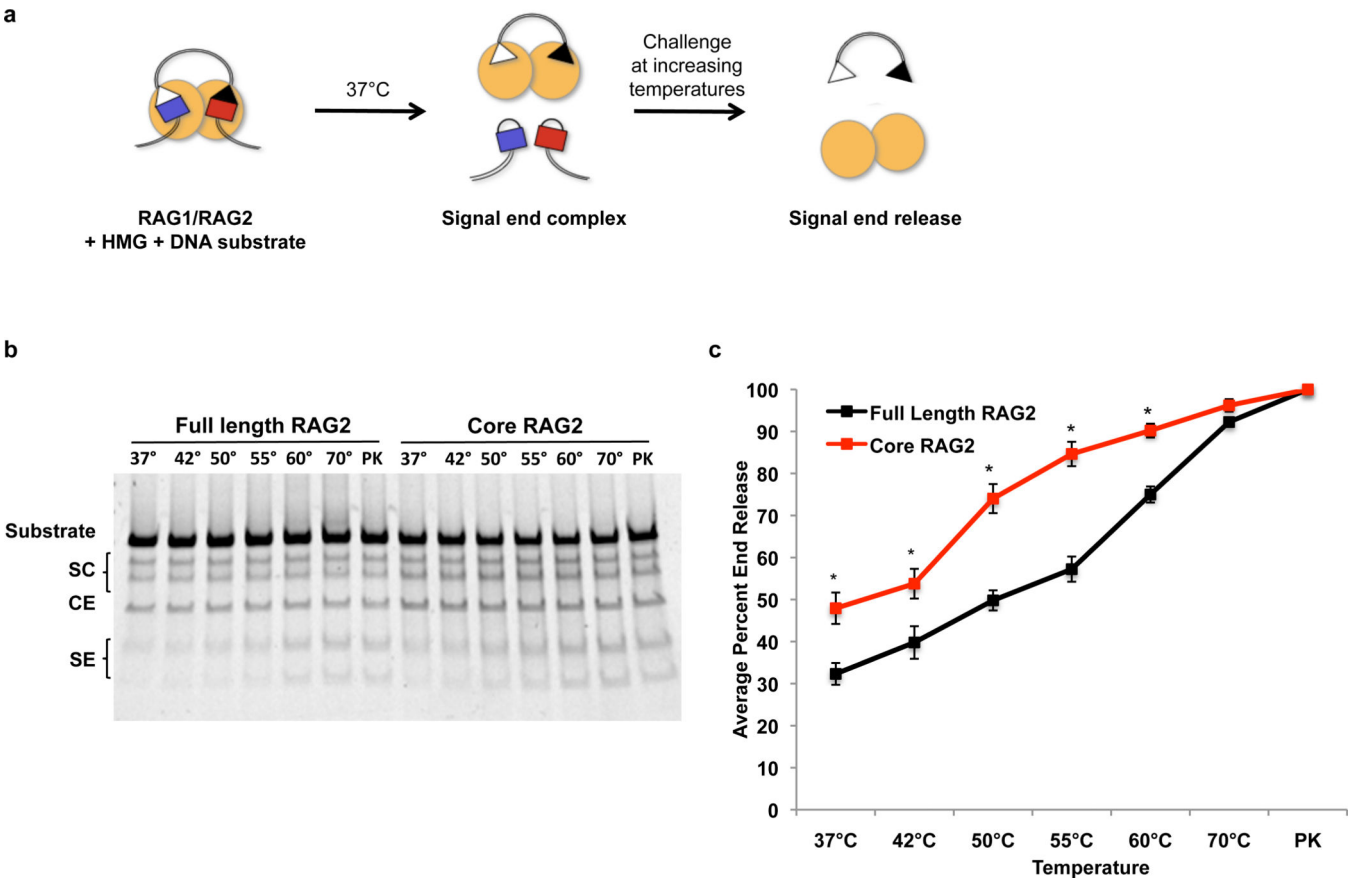

Figure 4. The C-terminus of RAG2 stabilizes the RAG post-cleavage complex

a. Biochemical end release assay. Purified GST-tagged core RAG1and non-tagged RAG2 (full length or core) proteins (yellow circles) cleave a 500bp DNA substrate at 37°C. Post-cleavage signal end complexes are thermally challenged at increasing temperatures to force the release of signal ends, which are detected after electrophoresis and gel staining. **b.** Representative gel for end release assays. Numbers above each lane indicate the temperatures the reactions were heated to before electrophoresis. PK, samples treated with proteinase K and SDS; SC, single cleavages; SE, signal ends; CE, coding ends. **c.** Quantification of SE release, measured as the combined amount of signal ends divided by the signal from the total amount of DNA in the lane, from six experiments using two different protein preparations (*$P < 0.05$, Student's t-test).